Observed features of the water masses in the Halmahera Sea in November 2016

Mochamad Riza Iskandar[1]*, Adi Purwandana[1], Dewi Surinati[1], Wang Zheng[2]

[1]*Research Center for Oceanography, Indonesian Institute of Sciences*
Jl. Pasir Putih 1, Ancol Timur, Jakarta 14430, Indonesia
[2]*Key Laboratory of Ocean Circulation and Waves, and Institute of Oceanology, Chinese Academy of Sciences*
7 Nanhai Road, Qingdao, Shandong 266071, China
Email: moch031@lipi.go.id

Abstract

Halmahera Sea is one of the locations in the eastern route of Indonesian Throughflow (ITF), where high salinity water is mainly transported by the ITF. The description of water mass in the Halmahera Sea from the perspective of water mass, and related mixing is important. It is not only useful for understanding water mass features, but it can also be used to determine the strength of the turbulent mixing, and so allow how it relates to the water transformation. Here, we report the water mass properties and estimation of mixing quantities in the Halmahera Sea from the CTD profiles based on recent onboard observations during the IOCAS cruise in November 2016. The water mass analysis was done by examining the characteristics of water types in the Temperature-Salinity (T-S) diagram. The mixing estimation uses the density profile derived from temperature and salinity profiles and the quantification of vertical turbulence observed by density overturn. Halmahera Sea is to be found as the location where the thermocline salinity changes abruptly, it is shown from the erosion of salinity maximum in the density of 22-26σ_θ decreased from the north to the south of the basin. It is associated with strong mixing with spots of higher vertical diffusivity in the thermocline and intermediate layer. In the upper layer, the mixed layer depth in the Halmahera Sea is relatively shallow with an average of about 16.95 m and it is associated with weak wind stress during this month.

Keywords: *Halmahera Sea, water masses, vertical mixing, cruise, salinity, temperature*

Introduction

The Indonesian Throughflow (ITF), pivotal ocean circulation in the Indonesian Seas, plays an important role in the heat and freshwater budget of the Pacific Ocean and Indian Ocean (Gordon, 1986; Lee *et al*., 2002). There are two main water routes connected the Pacific Ocean and the Indian Ocean via Indonesian Seas called the western and eastern routes. The western route extends from Sulawesi Sea, Makassar Strait until Lombok Strait and Banda Sea, meanwhile the eastern route extends from Halmahera Sea, Lifamatola Strait, and Banda Sea (Gordon, 2005; Tillinger and Gordon, 2009). The characteristics of water masses from the Pacific Ocean are transformed into nearly isohaline pattern when exits the Indonesian Sea (Koch-Larrouy *et al*., 2008, 2007). Each area along the ITF routes has a unique water mass signature shown in Temperature-Salinity (T-S) diagram, as an impact from the massive vertical mixing as well as large input of the freshwater (Ffield *et al*., 2000; Gordon and Susanto, 2001; Koch-Larrouy *et al*., 2008; Nagai and Hibiya, 2015; Nagai *et al*., 2017). Moreover, the monsoonal circulation also drives the water mass characteristics seasonally, especially in the upper layer (Qu *et al*., 2005; Du *et al*., 2008).

The shape of T-S diagram with the high salinity maximum in the thermocline layer from the Pacific Ocean changes drastically in the eastern route of ITF (Koch-Larrouy *et al*., 2007; Nagai *et al*., 2017). Nonetheless, the Halmahera Sea is the entry portal of water masses from the Pacific Ocean in the Indonesian Seas via the eastern route. It is important to describe the water mass characteristics in the Halmahera Sea from the perspective of water mass variations, quantification of the dissipation rate, and related turbulent mixing, because this location is one of the choke point of water mass transformation in the eastern route of ITF (Nagai and Hibiya, 2015). Estimation of turbulent energy dissipation rate, and vertical diffusivity is important for improving the existing ocean models that is needed to adjust climate modeling (Koch-Larrouy *et al*., 2010).

The water mass properties in Halmahera Sea has been discussed by several papers. For example, Koch Larrouy *et al*. (2007) from their model shows that the salinity maximum of the South Pacific water

*) Corresponding author

https://ejournal.undip.ac.id/index.php/ijms
DOI: 10.14710/ik.ijms.26.4.225-236
Received : 10-06-2021
Accepted : 01-09-2021

is eroded in the Halmahera Sea (Koch-Larrouy *et al*., 2007). Kashino *et al*. (2013) show that the mixed water between northern and southern hemispheres in the Halmahera Sea is related to the Halmahera eddy (Kashino *et al*., 2013). By using high-resolution non hydrostatic three-dimensional numerical experiments, Nagai *et al*. (2017) found the rigorous vertical mixing is induced by breaking of internal tides in the shallow regions of the Halmahera Sea, which further dilutes the ITF waters. By using Conductivity-Temperature-Depth (CTD) cast during INDOMIX cruise in July 2010, Koch Larrouy *et al*. (2015) (hereafter called KL15) found the high dissipation rate is related to strong mixing processes of different water masses in the Halmahera Sea (Koch-Larrouy *et al*., 2015). They show a wide range of dissipation values from their estimation that nearly agree with vertical distribution estimation of natural radionuclides. Surinati *et al*. (2021) found that the Pacific waters are characterized by the strong salinity stratification in the 0–300m depth, and to be found it is influenced by precipitation rate. However, Surinati *et al*. (2021) estimate the water masses only in the entry transect of the Halmahera Sea and do not concerns about the mixing quantities. Therefore, in this paper, we extends the research from Surinati *et al*. (2021) and KL15 by describing the water masses features with the full coverage of CTD stations during cruise in the entire Halmahera Sea at the end of the second transition monsoon in 2016, and also provides the estimation of mixing quantities from the CTD profiles.

Materials and Methods

The Research Center for Oceanography, Indonesian Institute of Sciences (RCO-LIPI) with the Institute Oceanology China Academy of Sciences (IOCAS) conducted a cruise in the eastern Indonesian Seas in November 2016. This cruise was held at the end of the second monsoon transition with a total 79 station cast and 8 mooring sites extending from Makassar Strait to the inflow ITF region in the Pacific Ocean (not shown in this paper). Although various types of ocean observations were conducted during this cruise, for this study, we use data from a CTD profiler (SBE 911 plus by Sea Bird Electronics) with the accuracy and resolution of temperature (conductivity) sensor at 0,001°C and ±0,0002°C (±0,0003 $S.m^{-1}$ and ±0,00004 $S.m^{-1}$) respectively. The dissolved oxygen data recorded from CTD is also used in this study, with the accuracy and resolution of the dissolved oxygen sensor at 1 μ mol kg^{-1} and 2% of saturation. The CTD is down cast with a maximum rate at 24 Hz. Because this study will investigate the water masses in the Halmahera Sea, we use 21 CTD casts for the dataset in the several transects as shown in Figure 1.

There are four transects representing the entire Halmahera Sea. The first transect is located in the north of Halmahera Sea, which is the entry portal of the Halmahera Sea in the eastern ITF route, the second transect is located in the southern part at the exit portal of Halmahera Sea, the third transect is in the central region crossing the north and south transect, and the fourth transect is located in the western side of Halmahera Sea at the small gap between Obi and Misool islands (see Figure 1.). There are 9 CTD stations in the north transect, 5 CTD stations in the south transect, 5 CTD stations in the central transect, and 4 CTD stations in the west transect. The number of CTD casts and maximum pressure (depth) for each transect can be seen in Table1.

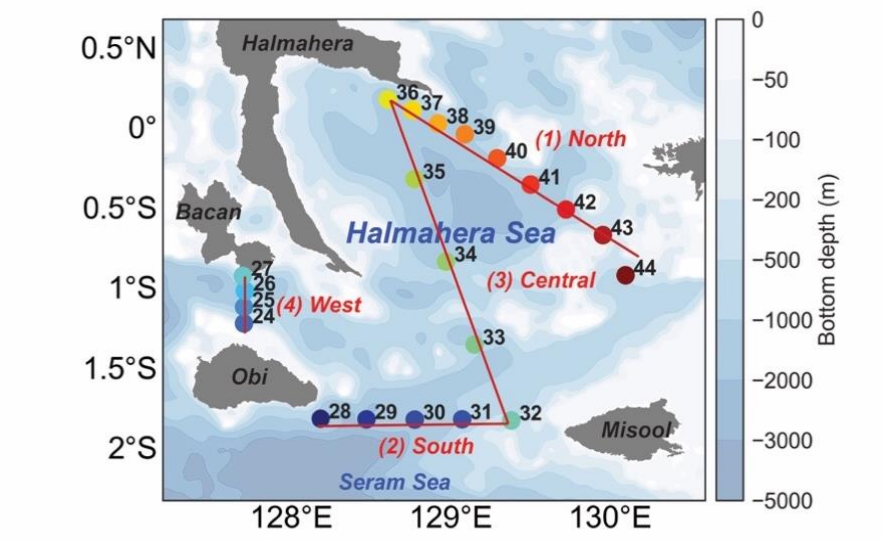

Figure 1. Sampling location of four transects including the (1) north, (2) south, (3) central, and (4) west transect in the Halmahera Sea, November 2016

Table 1. Number of CTD casts and maximum depth for each transect in Halmahera Sea used in this study

Transect	Station number	Maximum CTD pressure (dB)
(1) North	36	1504
	37	1404
	38	1304
	39	779
	40	529
	41	1354
	42	1254
	43	904
	44	629
(2) South	28	1504
	29	1514
	30	879
	31	804
	32	455
(3) Central	32	455
	33	679
	34	1104
	35	1854
	36	1504
(4) West	24	429
	25	1329
	26	1329
	27	829

Table 2. Properties of water masses defined in this study

Water Type	Characteristics	T (°C)	S (psu)	O_2 (ml l^{-1})
South Pacific Subtropical Water (SPSW)	Salinity maximum	19–27	35.0–35.6	3.0–3.5
South Pacific Intermediate Water (SPIW)	Salinity minimum, O_2 minimum	5.0–7.0	34.45–34.60	1.9–3.0

The Temperature-Salinity (T-S) diagram is used to defines the water mass characteristics in the Halmahera Sea. A data subset for the T-S Diagram is selected by requiring each retained station that has temperature, salinity, and dissolved oxygen data. The water type is done by examining the water mass characteristics defined by Wyrtki (1961). See Table 2. The temperature and salinity (T-S) fields on each station are used to derive the potential density anomaly relative to surface depth (σ_θ). Potential density anomaly in the TS diagram is estimated by Gibbs SeaWater Oceanographic Package of TEOS-10 (McDougall and Barker, 2011).

For the mixing estimates, this study follows the method from Purwandana *et al*. (2020)by using the density profile derived from temperature and salinity profiles (Purwandana *et al*., 2020). The quantification of vertical turbulence observed by density overturns following the method by Thorpe (1977). The improvement of the Thorpe method by Purwandana *et al*. (2020) is used to estimate the TKE dissipation rates. The TKE (ε) and turbulent diffusivity (K_ρ) are estimated as,

$$\varepsilon = \varepsilon_{Th-GM} = \begin{cases} 0.64 {L_T}^2 N^3, & when\ overturn\ observed \\ \max\left(1 \times 10^{-10}, \varepsilon_o \left(\frac{N^2}{{N_o}^2}\right)\right), & no\ overturn \end{cases}$$

$$K_\rho = K_{\rho\, Th-GM} = \Gamma \frac{\varepsilon_{Th-GM}}{N^2}$$

Note : L_T is the Thorpe length scale calculated by root mean square value of vertical displacement, N is the buoyancy frequency, 1×10^{-10} is the lowest dissipation rate observed by microstructure measurements in the Indonesian Seas (Banda Sea (Koch-Larrouy *et al*., 2015; Bouruet-Aubertot *et al*., 2018;)); ε_0 is the canonical Garret and Munk dissipation rate set as 7×10^{-10} m^2 s^{-3} , N_0 is buoyancy frequency reference, set as 3 cph, and $\Gamma = 0.2$ is the mixing efficiency.

The Mixed Layer Depth (MLD) of each profile follows the method from de Boyer Montégut *et al*. (2004). The MLD is estimated on individual CTD profiles that are defined through the threshold method with a finite-difference criterion from a near-surface reference. The reference depth is set at 5 m,

the chosen temperature and density differences are 0.2°C and 0.03 kg.m^3, respectively. The minimum MLD between temperature and density criterion is used as the MLD at each CTD data profile. We also estimate the wind stress in the Halmahera sea from wind velocity fields that are provided by European Centre for Medium-Range Weather Forecasts (ECMWF) Reanalysis v5 (ERA5) (Dee *et al*., 2011). Wind stress is calculated by $\tau = \rho_{air} C D u^2$, where t is the vector wind stress, ρ_{air} is the density of air (1225 kg m^{-3}), CD is the drag coefficient by Yelland and Taylor (1996), and u is wind velocity. (ERA5 was accessed at https://cds.climate.copernicus.eu/cdsapp#!/dataset/reanalysis-era5-single-levels-monthly-means?tab=form, on 23 July 2021).

Result and Discussion

Structure of water masses

Figures 2a and Figure 2b are the T-S diagrams from all stations as the function of pressure and dissolved oxygen (DO), respectively. This plot is used to look at the characteristics of water masses at a range of temperature and salinity. The water types in terms of their characteristics in the range of temperature, salinity, and dissolved oxygen can be found in Table 2. These water characteristics are based on Wyrtki (1961).

The water in the density of less than 22σ_θ is characterized by a high temperature of about 25-30^{o}C, in a depth of less than 50m, and a low salinity range of less than 34psu. It is also associated with very high dissolved oxygen of more than 3.75 ml.L^{-1}. These are the common characteristics of surface water, where the dissolved oxygen is remarkably high because it closes the atmosphere.

In the thermocline layer, at a density range of about 23-26σ_θ or around 100-400m, there is a wide range of salinity with the salinity maximum of around 35 psu, and a temperature range of about 15-23^{o}C (Figure 2a.). The DO in this depth varies in a range of 3.00–3.5 ml.L^{-1} (Figure 2b.). From these characteristics, based on Table 2, the water type in this layer is known as South Pacific Subtropical Water (SPSW). Some paper also argue that this water mass is the South Pacific Subtropical Water (SPSW) (Koch-Larrouy *et al*., 2007; Surinati *et al*., 2021), it also often called South Pacific Tropical Water (SPTW) (Gordon, 2005; Koch-Larrouy *et al*., 2015). Nonetheless, the SPSW (or SPTW) formed in the eastern tropical South Pacific Ocean, where the evaporation is larger than precipitation, and as it subducted and advected from the source, the salinity maximum will be eroded due to ocean physics processes (Qu *et al*., 2013; Yang *et al*., 2018). Even though the salinity range is not the same as it is in the formation region, the salinity maximum characteristics still appear in the Halmahera Sea as a remnant of SPSW.

The wide range of salinity in the T-S diagram in the Halmahera Sea could also represent the strong mixing, where it changes salinity characteristics in a relatively small basin. Furthermore, the horizontal advection also leads to the erosion of the salinity maximum as the ITF flowing through these passages (Surinati *et al*., 2021). The numerical approaches from KL15 found the tidal mixing erodes SPSW salinity maximum for more than 0.4 psu were identified when the water mass enters the Halmahera Sea.

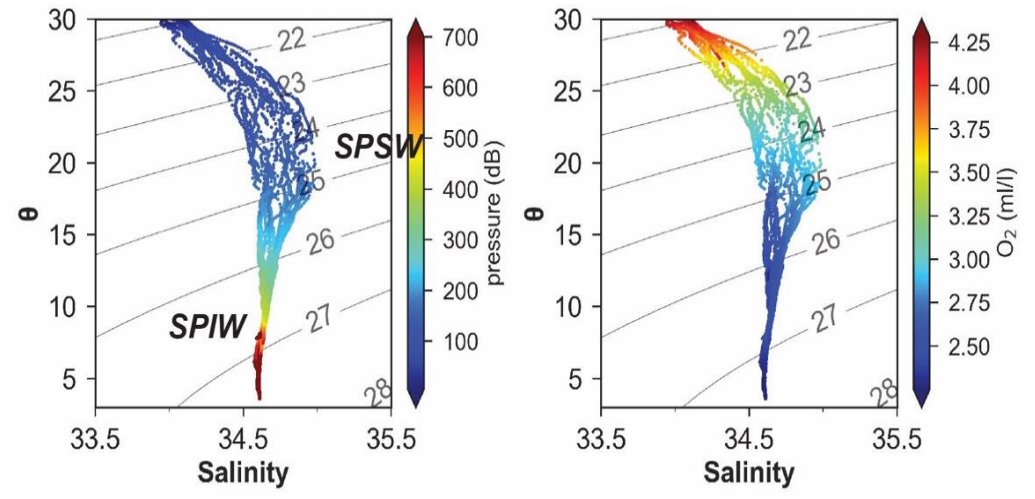

(a) (b)

Figure 2. TS Diagram as a function of (a) pressure (dB) and (b) O_2 (ml.L^{-1}). The water type of South Pacific Subtropical Water (SPSW) and South Pacific Intermediate Water (SPIW) is noted.

In the intermediate layer (density range, 26-27.3σ_θ, more than 500m), both salinity and DO are nearly constant around 34.52 psu and 2.50 ml.L^{-1} respectively. These characteristics are the remnant of South Pacific Intermediate water (SPIW) (Table 2,). (Wyrtki, 1961) found this intermediate characteristic in the eastern basin of Indonesian seas.

Potential density anomalies and T-S profiles

The water masses investigated during the IOCAS cruise using CTD profiles show an interesting transformation of salinity maximum water in the Halmahera Sea. The hydrological profiles measured during the IOCAS cruise in the T-S diagram are plotted separately on each transect that is located following the entrance of the Halmahera Sea until the end of the sea before it reaches the Seram Sea (Figure 1.). Figure 3 represents the density profile and T-S diagram of each station from all transects. It shows that step-like features in the density profiles are observed in almost all transects, suggesting strong mixing of water masses occur in the sea (Figure 3 upper panel). The step-like features are found of about the thermocline depth from 30 to and reach up to 120 m (Figures 3a, 3b, and 3c.). Nonetheless, the step-like features are not much found at the stations in the west transect (Figure 3d.) compared to the other stations. KL15 found a large variability of the density profiles over one day period in this location. These strong step-like features in this location may result from large local mixing events or vertical displacement of the isopycnals due to internal tide propagation or the advection from Halmahera eddy. Nonetheless, these step-like features are not large as KL15 found in July 2010, suggested that the data used in this study is a snapshot CTD sampling that is not continued sampled in each station, so it is hard to capture when the internal tide occurs.

The middle panel of Figure 3 shows T-S diagram profiles on each transect. The SPSW is characterized by salinity maximum (>35 psu) that fills the thermocline, whereas the lower salinity

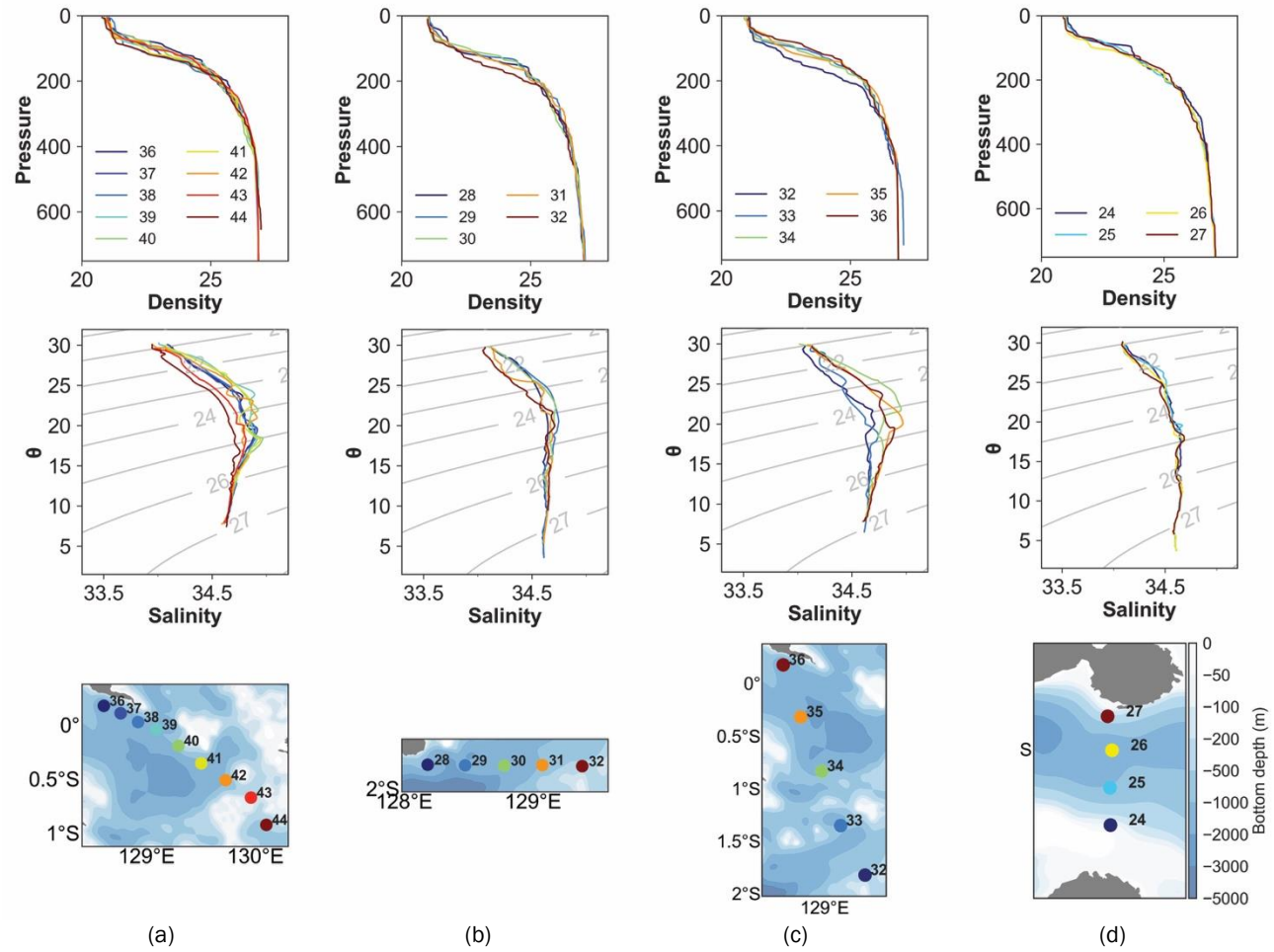

Figure 3. TS Diagram of the a) north, b) south, c) central and d) west transect in the Halmahera Sea, November 2016.

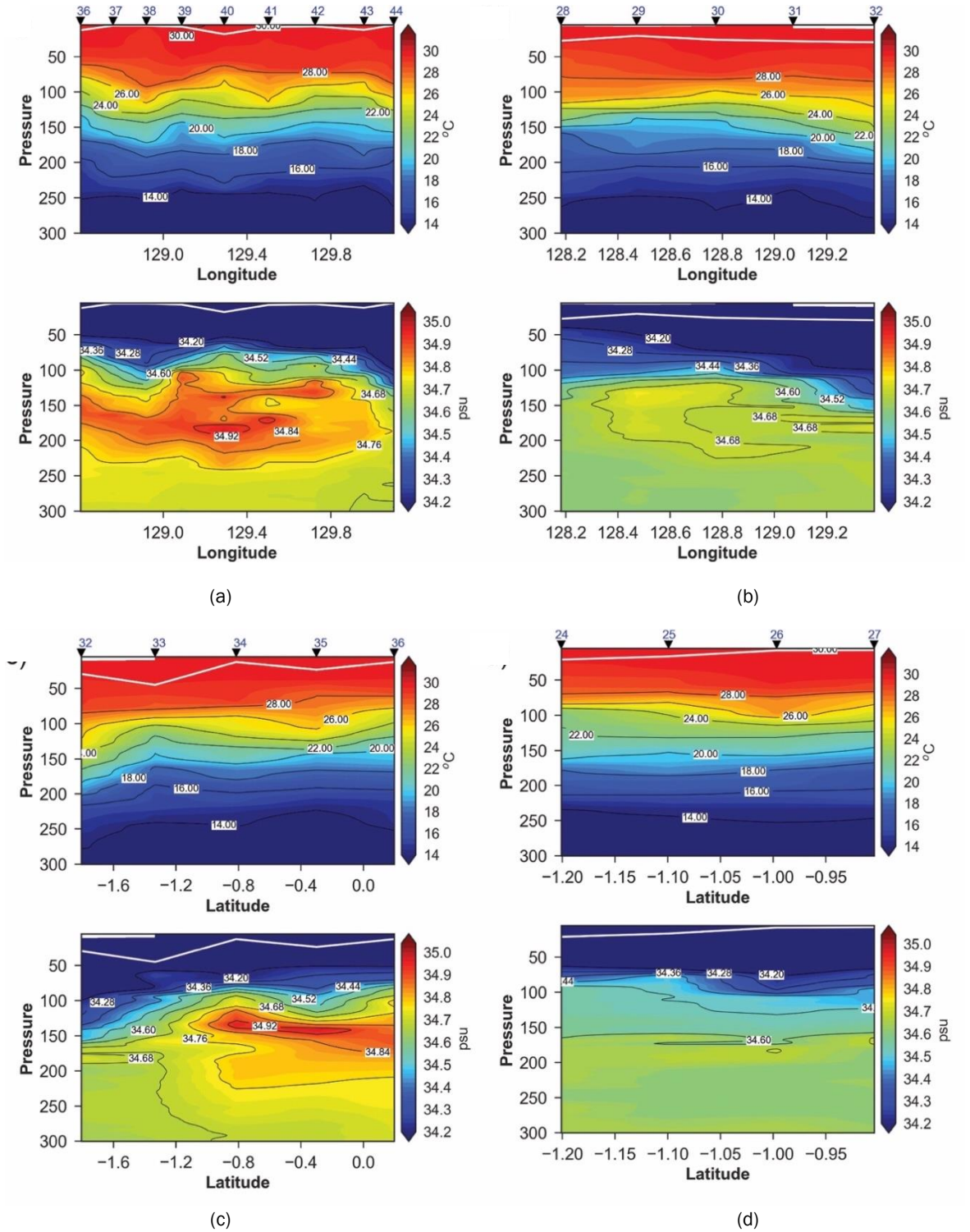

Figure 4. The temperature (T) and salinity (S) of the a) north, b) south, c) central, and d) west transect in the Halmahera Sea, November 2016. Black contour represents interval of salinity (0.08 psu) and temperature (2°C) respectively. White contour represents the mixed layer depth determined by the CTD profile using temperature and density criterion at 0.2°C and 0.03 kg/m^3 respectively.

characteristic SPIW is found in the intermediate levels. KL15 also observe a different salinity maximum in one day period on the TS diagram. They suggest the different salinity maximum in a relatively short period are occurred due to a local process such as the presence of internal tides. It shows that the

high salinity water in the thermocline on the TS diagram (23-26σ_θ) is eroded that show gradually fresher from the north to the south transect. The gradual erosion of salinity in the thermocline is more pronounced in the central transect. It also shows that the T-S diagram in the west transect and south transect are similar. This represents that the water masses in both transects have transformed that shows as a relatively isohaline profile from thermocline to intermediate depth. KL15 found the salinity maximum of the South Pacific water is strongly eroded as soon as it enters the Halmahera Sea. The salinity maximum was also reduced when crossing the Seram Sea and the Buru Strait. Because of upstream transformation occurred, the signature of the strong salinity maximum of the subtropical water has almost completely disappeared in the Banda Sea (Koch-Larrouy *et al*., 2015).

Stratification of water masses

Figure 4 shows the stratification of temperature (T) and salinity (S) sections along four transect lines during the IOCAS cruise that was conducted at the end of the second transition monsoon from surface to 300 m. The transect map is set to the maximum of 300 m to look at the gradual erosion of salinity in the thermocline depth. The highest salinity maximum is more pronounced in the north transect (Figure 4a.) suggesting the salinity that not much changes from its sources in the Pacific Ocean. In the north transect within the surface to 50 m depth, salinity is below 34.3 psu. Below this depth, between depths of 100 and 250 m along lines, a salinity maximum occurred with salinity values exceeded 34.9 psu, except in station 44 with salinity less than 34.6 psu. Salinity maximum is concentrated around 180 m depth. This water is considered as the remnant of SPSW originating from the South Pacific (Tsuchiya *et al*., 1989). Lower salinity water than 34.5 psu is observed beneath this SPSW (Figures 2 and 3 on the TS diagram). Kashino *et al*. 2013 was also observed the high salinity water from the South Pacific around 1-5°N in the Halmahera eddy region just in the north of the first transect. Kashino *et al*. (2013) also suggest that the Halmahera eddy region is the location of the water masses from both hemispheres are sandwiched together. Low-salinity water originating from the North Pacific is carried south by the Halmahera Eddy (Kashino *et al*., 2013).

The south transect is located in between Obi and Misool Islands in the south of the Halmahera Sea. In this location, between depth of 100 and 250m, there is no more signature of salinity maximum like in the north transect (Figure 4b.), it is shown from the salinity in this depth range that is less than 34.6 psu (compare to the salinity maximum in the north transect of about 35.0 psu). It is indicated that the salinity maximum water from the Pacific Ocean have transformed into the fresher characteristic as shown in the south transect. Furthermore, it is suggested that the water could have experienced mixing before reaches this location.

The central transect is located in the middle of the Halmahera Sea crossing the north and south transect as can be seen in Figure 4c. Interestingly, in this location, the signature of salinity maximum at depth of 100 and 300 m still can be observed in the north part at stations 34, 35, 36, similar to the first transect in the north of Halmahera Sea (Figures 3a and 4a.). In the south part at stations 32 and 33 the signature of salinity maximum at depth of 100 m and 300 m is not observed, the salinity properties in these two-stations are similar to the second transect (Figures 3b and 4b.). This indicate that the water mass transformation that changes the high salinity water to the fresher characteristics at the thermocline depth occurrs in this region.

The west transect is located in the small gap between Obi and Bacan Islands. The salinity at depths of 100 and 300 m in this transect is similar to the south transect, whereas the salinity maximum at the thermocline is not as large as the north transect (Figures 3d and 4d.). This could indicate that the high salinity water has transformed before reaches this location. The Halmahera Sea act as a transformation region of the salinity changes in the thermocline depth. Generally, the Halmahera Sea is the location where the strong mixing occurred, as can be seen in the density profile that shows the step-like profiles in almost all stations.

Estimates of turbulent mixing

As in the previous section, estimates of the mixing quantities *i.e*., turbulent kinetic energy dissipation rate (ε, m^2s^{-3}) and vertical eddy diffusivity ($K\rho$, m^2s^{-1}) are estimated by density overturn method. Figure 5 shows the turbulent kinetic energy dissipation rate and vertical eddy diffusivity on each station in all transects. Generally, it shows that a large dissipation rate is confined in the depth of 80-500m, or the thermocline layer, and vertical eddy diffusivity also varied in that depth range. In the first 60 m, vertical eddy diffusivity looks high, which characterizes the surface mixed layer. KL15 suggests there is no evidence of additional mixing due to internal tides in the upper 60m. The high vertical eddy diffusivity is also observed in the depth range of 600-1000m or in the intermediate layer, which increases with ocean depth. Nonetheless, it is more pronounced in the north and central transects (Figures 5a and 5c.), compared to the south and west transect (Figures 5b and 5d.). Conclude, where stratification decreases, the $K\rho$ values generally

increase with depth, being more than 2 orders of magnitude higher in the intermediate or deep layer. KL15 assumes this profile are found to be associated with a lot of internal tides that are generated above the straits. So that, as stratification decreases, the set is noticed to be very strong and *Kρ* increasing with depth.

Comparing all transect, the high variability of turbulent kinetic energy dissipation rate and vertical eddy diffusivity is observed in almost all stations in the north transect, not only is it noticed in the thermocline but also the intermediate layer, with *Kρ* values mostly above 10^{-4} m^2s^{-1}. Suggested, the water masses experience strong vertical mixing, when it first enters the basin.

The T-S map shown in Figure 6 determines the mixing characteristics within a specific density range of the waters in Halmahera Sea vertically. The gridded T-S plot of TKE dissipation rate and vertical eddy diffusivity derived from cruise CTD profiles shown in Figure 5a and b respectively, which is done by plotting T-S diagram in 0.2°C × 0.05 psu space. There is a higher ε= 10^{-8}-10^{-7} m^2s^{-3} dissipative layer (24-27σ_θ or a depth of more than 100 m) in the lower thermocline and the intermediate layer (Figure 4a.). Cuypers *et al*., 2017 found a higher dissipation rate is usually observed in the thermocline due to the refraction effect of stratification that focuses on the energy of internal tide (Cuypers *et al*., 2017; Purwandana and Iskandar, 2020). A lower dissipation rate is found in the upper and lower layers. The vertical diffusivity follows the pattern of the dissipation rate, as the decreasing stratification, the value increases at depth (Figure 4b.). Generally, the energy dissipation in the thermocline of Halmahera Sea is quite high. These mixing quantities values compare well with previous estimates using yoyo CTD and instantaneous estimates by using microstructure profiler in Halmahera Sea from KL15.

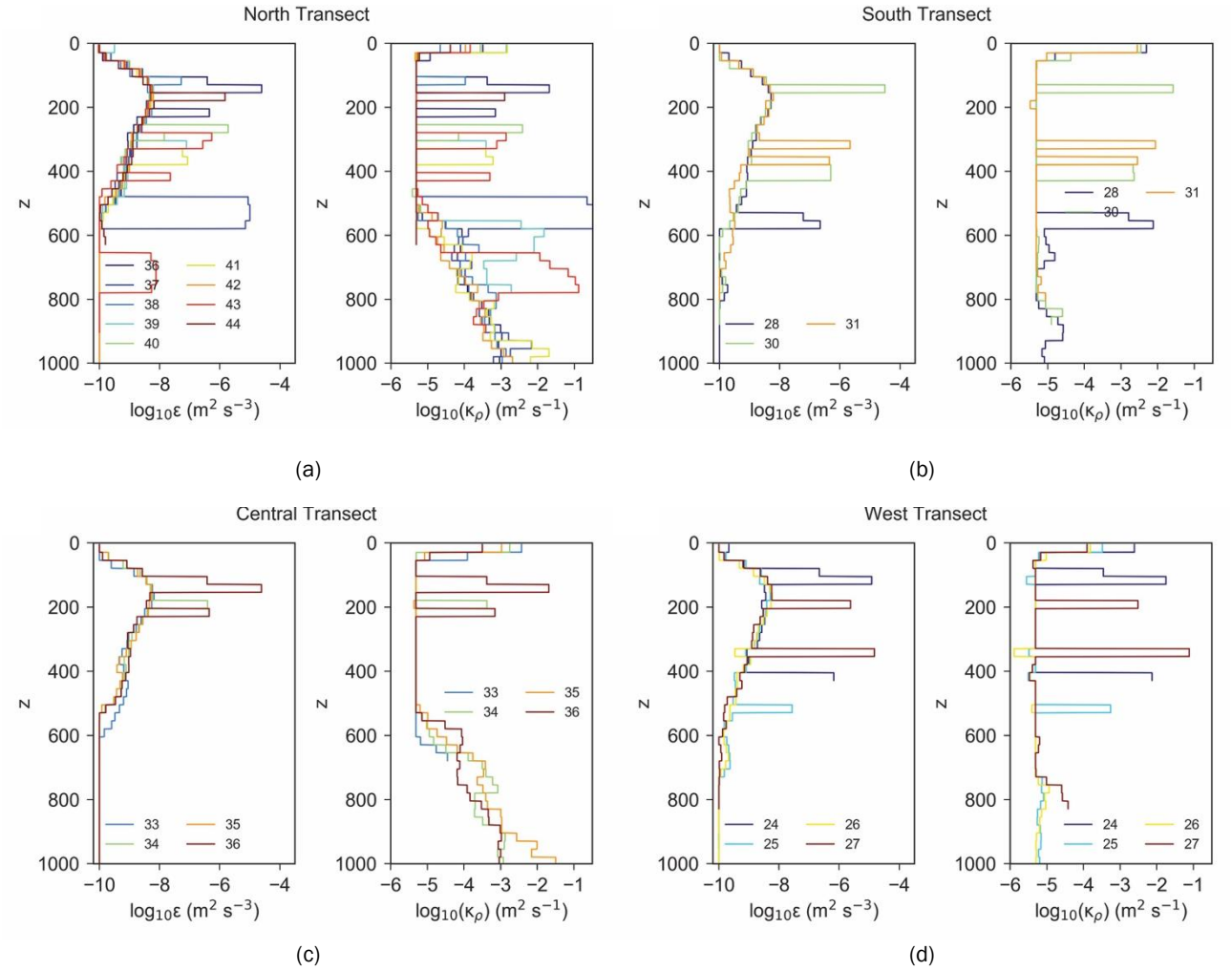

Figure 5. Profiles of turbulent kinetic energy dissipation rate (in $\log_{10}$ scale ε, m^2s^{-3}) and vertical eddy diffusivity (in $\log_{10}$ scale *Kρ*, m^2s^{-1}) on each station in a) North, b) South, c) Central, and d) West transects. Note that several profiles do not appear due to error calculation.

Mixed layer depth

The surface mixed layer is a layer where this turbulence is generated by mechanical forcing from winds, as well as buoyancy forcing. The MLD determination in this study is done by using threshold values in the temperature and density criteria. Figure 7 shows the MLD at each station during the cruise. We found the MLD in the Halmahera Sea is relatively shallow, with an average of MLD from all stations in November 2016 is about 16.95±10.18 m. The deepest MLD is found at station 33 (45m) and shallowest at station 44 (5 m). Even though there is a similar pattern of temperature and salinity profiles compare to KL15 result in July 2010, we can't compare the mixed layer depth in this study with the result from KL15 in July, since there isn't information of mixed layer depth given in the previous study. Nonetheless, (Radjawane *et al*., 2015) found that the MLD in the north of Papua Island, the location of eastern inflow of ITF in the upstream of Halmahera Sea, is found to be shallower during transition monsoon and deeper during summer monsoon with the maximum in July, they suggest the MLD corresponds to the changes of wind speed.

By looking at the wind stress from the monthly ERA5 dataset in the Halmahera Sea (127.5°-130.5°E; 2°S-2°N) in 2016 (Figure 8.), generally shows, during transition monsoon (both MAM and SON), weaker wind stress is observed compared to the northwest (DJF) and southeast monsoon (JJA). It is found that the maximum wind stress occurs in August 2016, whereas the minimum in May 2016. We also found that the wind stress is weak in November 2016, that is could be the main responsible factor that forces shallow MLD in the Halmahera Sea.

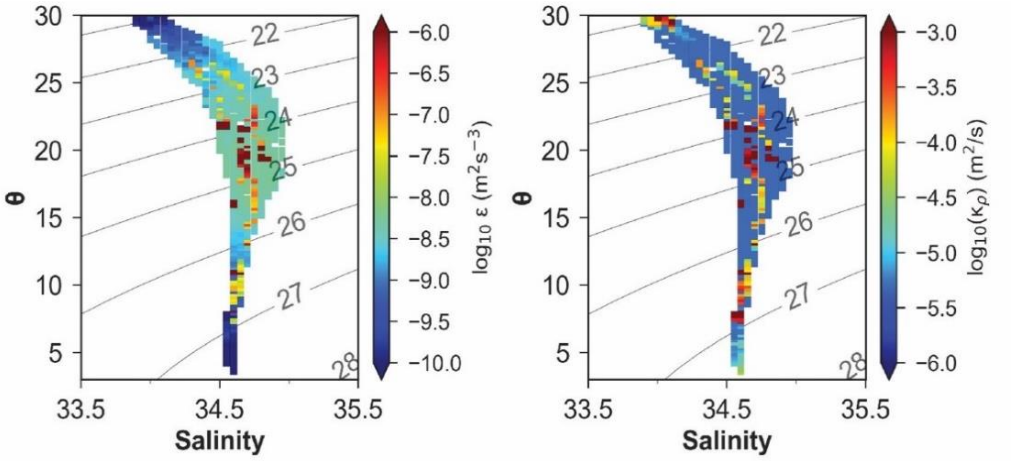

Figure 6. Grid averaged TS diagram in 0.2°C × 0.05 psu space of the (a) turbulent kinetic energy dissipation rate (in $\log_{10}$ scale ε, m^2s^{-3}) and (b) vertical eddy diffusivity (in $\log_{10}$ scale $K\rho$, m^2s^{-1}).

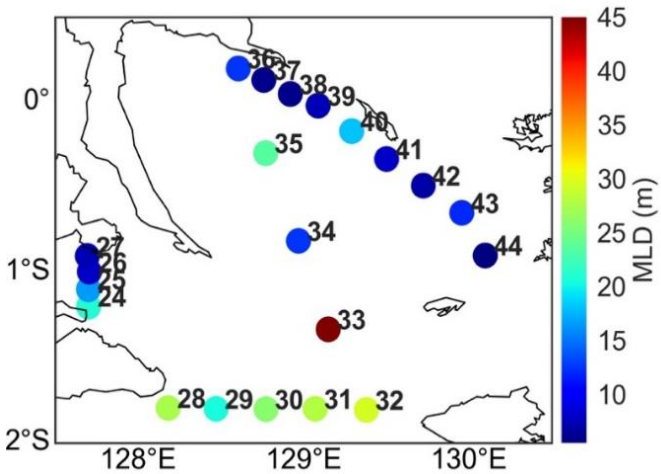

Figure 7. Mixed layer depth each station during cruise.

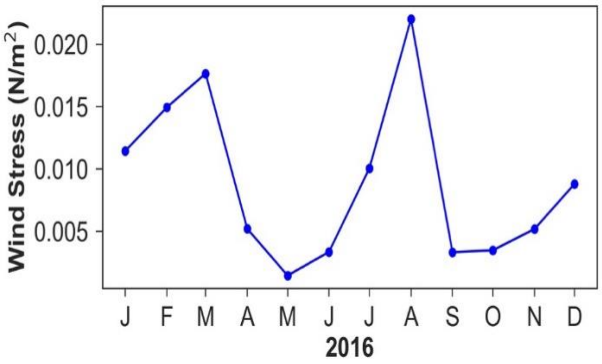

Figure 8. Monthly mean of wind stress in Halmahera Sea (127.5°-130.5°E; 2°S-2°N). Wind stress is calculated from ERA5.

Conclusion

The water masses in the Halmahera Sea show a unique pattern, it is found that there are two distinct water masses called with South Pacific Subtropical Water in the thermocline that is characterized by the salinity maximum, and South Pacific Intermediate Water that is characterized by salinity minimum. This study also found that the salinity maximum is more pronounced in the north transect, compared to the south transect, as well as the west transect. This implies that, when water masses pass through the basin, the salinity maximum will be eroded by an oceanic process such as turbulent vertical mixing. It is also shown that there is a step-like density profile that exists in almost all transects, thus further suggests a strong mixing process. Moreover, this study found enhanced dissipation rates and vertical diffusivity in the thermocline and intermediate layer ($\varepsilon>10^{-8} m^2s^{-3}$; $K_\rho>10^{-4} m^2s^{-1}$) which might be strongly related to the internal tides. The step-like feature was also found in the previous onboard result from KL15 with a similar dissipation rate range at 10^{-7} m^2s^{-3} to 10^{-4} m^2s^{-3}. The Halmahera Sea is one of the mixing hotspots in the Indonesian Seas that is related to rough topography on narrow passages. It is also observed that the MLD is shallow during the cruise, which could be influenced by weak wind stress.

Acknowledgment

Thanks to the reviewer for the constructive comments, so that this paper can be published. We would like to thank the crew of R/V Baruna Jaya VIII and all the scientific and technical crew on board. IOCAS and RCO-LIPI provided technical and financial support for the IOCAS cruise. MRI and AP are the main contributors in this manuscript, while DS and WZ are the supporting contributors. This project is funded by research scheme of Program Riset Unggulan COREMAP CTI 2021-2022 (17/A/DK/2021).

References

Bouruet-Aubertot, P., Cuypers, Y., Ferron, B., Dausse, D., Ménage, O., Atmadipoera, A. & Jaya, I., 2018. Contrasted turbulence intensities in the Indonesian Throughflow: a challenge for parameterizing energy dissipation rate. *Ocean Dyn*. 68: 779–800. doi: 10.1007/s10236-018-1159-3

Cuypers, Y., Bouruet-Aubertot, P., Vialard, J. & McPhaden, M.J., 2017. Focusing of internal tides by near-inertial waves. *Geophys. Res. Lett.* 44: 2398–2406. doi: 10.1002/2017GL072625

de Boyer Montégut, C., Madec, G., Fischer, A.S., Lazar, A. & Iudicone, D., 2004. Mixed layer depth over the global ocean: An examination of profile data and a profile-based climatology. *J. Geophys. Res. C Ocean.* 109: 1–20. doi: 10.1029/2004JC002378

Dee, D.P., Uppala, S.M., Simmons, A.J., Berrisford, P., Poli, P., Kobayashi, S., Andrae, U., Balmaseda, M.A., Balsamo, G., Bauer, P., Bechtold, P., Beljaars, A.C.M., van de Berg, L., Bidlot, J., Bormann, N., Delsol, C., Dragani, R., Fuentes, M., Geer, A.J., Haimberger, L., Healy, S.B., Hersbach, H., Hólm, E. V, Isaksen, L., Kållberg, P., Köhler, M., Matricardi, M., McNally, A.P., Monge-Sanz, B.M., Morcrette, J.J., Park, B.K., Peubey, C., de Rosnay, P., Tavolato, C., Thépaut, J.N. & Vitart, F. 2011. The ERA-Interim reanalysis: configuration and performance of the data assimilation system. *Q. J. R. Meteorol. Soc.* 137: 553–597. doi: 10.1002/qj.828

Du, Y., Qu, T. & Meyers, G., 2008. Interannual Variability of Sea Surface Temperature off Java

and Sumatra in a Global GCM. *J. Clim*. 21, 2451–2465. doi: 10.1175/2007jcli1753.1

Ffield, A., Vranes, K., Gordon, A.L., Dwi Susanto, R. & Garzoli, S.L., 2000. Temperature variability within Makassar Strait. *Geophys. Res. Lett.* 27: 237–240. doi: 10.1029/1999GL002377

Gordon, A.L., 2005. Oceanography of the Indonesian Seas and Their Throughflow . *Oceanography* 18: 14-27.

Gordon, A.L., 1986. Interocean exchange of thermocline water. *J. Geophys. Res*. 91: 5037. doi: 10.1029/JC091iC04p05037

Gordon, A.L. & Susanto, R.D., 2001. Banda Sea surface-layer divergence. *Ocean Dyn.* 52: 2–10. doi: 10.1007/s10236-001-8172-6

Kashino, Y., Atmadipoera, A., Kuroda, Y. & Lukijanto, 2013. Observed features of the Halmahera and Mindanao Eddies. *J. Geophys. Res. Ocean*. 118: 6543–6560. doi: 10.1002/2013JC009207

Koch-Larrouy, A., Atmadipoera, A., van Beek, P., Madec, G., Aucan, J., Lyard, F., Grelet, J. & Souhaut, M., 2015. Estimates of tidal mixing in the Indonesian archipelago from multidisciplinary INDOMIX in-situ data. *Deep Sea Res. Part I Oceanogr. Res. Pap*. 106: 136–153. doi: 10.1016/j.dsr.2015.09.007

Koch-Larrouy, A., Lengaigne, M., Terray, P., Madec, G. & Masson, S., 2010. Tidal mixing in the Indonesian Seas and its effect on the tropical climate system. *Clim. Dyn*. 34: 891–904. doi: 10.1007/s00382-009-0642-4

Koch-Larrouy, A., Madec, G., Bouruet-Aubertot, P., Gerkema, T., Bessières, L. & Molcard, R., 2007. On the transformation of Pacific Water into Indonesian Throughflow Water by internal tidal mixing. *Geophys. Res. Lett.* 34: 1–6. doi: 10.1029/2006GL028405

Koch-Larrouy, A., Madec, G., Iudicone, D., Atmadipoera, A., Molcard, R., 2008. Physical processes contributing to the water mass transformation of the Indonesian throughflow. *Ocean Dyn*. 58: 275–288. doi: 10.1007/s10 236-008-0154-5

Lee, T., Fukumori, I., Menemenlis, D., Xing, Z. & Fu, L.L., 2002. Effects of the Indonesian Throughflow on the Pacific and Indian Oceans. *J. Phys. Oceanogr.* 32: 1404–1429. doi: 10.1175/ 1520-0485(2002)032<1404:eotito>2.0.co;2

McDougall, T.J. & Barker, P.M., 2011. Getting started with TEOS-10 and the Gibbs Seawater (GSW) Oceanographic Toolbox. SCOR/IAPSO WG127.

Nagai, T. & Hibiya, T., 2015. Internal tides and associated vertical mixing in the Indonesian Archipelago. *J. Geophys. Res. Ocean*. 120: 3373–3390. doi: 10.1002/2014JC010592

Nagai, T., Hibiya, T. & Bouruet-Aubertot, P., 2017. Nonhydrostatic Simulations of Tide-Induced Mixing in the Halmahera Sea: A Possible Role in the Transformation of the Indonesian Throughflow Waters. *J. Geophys. Res. Ocean.* 122: 8933–8943. doi: 10.1002/2017JC013381

Purwandana, A., Cuypers, Y., Bouruet-Aubertot, P., Nagai, T., Hibiya, T. & Atmadipoera, A.S., 2020. Spatial structure of turbulent mixing inferred from historical CTD datasets in the Indonesian seas. *Prog. Oceanogr.* 184: 102312. doi: 10.1016/j.pocean.2020.102312

Purwandana, A. & Iskandar, M.R., 2020. Turbulent Mixing Inferred from CTD Datasets in the Western Tropical Pacific Ocean. *Ilmu Kelautan: Indonesian Journal of Marine Science,* 25(4): 148-156. doi: 10.14710/ik.ijms.25.4.148-156

Qu, T., Du, Y., Strachan, J., Meyers, G. & Slingo, J., 2005. Sea Surface Temperature and its Variability in the Indonesian Region. *Oceanography,* 18: 50–61. doi: 10.5670/oce anog.2005.05

Qu, T., Gao, S. & Fine, R., 2013. Subduction of South Pacific Tropical Water and Its Equatorward Pathways as Shown by a Simulated Passive Tracer*. *J. Phys. Oceanogr.* 43: 1551–1565. doi: 10.1175/JPO-D-12-0180.1

Radjawane, I.M., Nurdjaman, S., Apriansyah, 2015. Seasonal variability of mixed layer depth in Indonesian Seas. *AIP Conf. Proc.* p1677. doi: 10.1063/1.4930690

Surinati, D., Corvianawatie, C., Kusmanto, E., Budiman, A.S., Bayhaqi, A., Avianto, P., Wardana, A.K., Purwandana, A., Ismail, M.F.A., Arifin, Z. & Yuan, D. 2021. The Variability of Upper-Ocean Salinity in the Eastern Inflow Region of ITF. I*OP Conference Series: Earth and Environmental Science,* 789(1): p. 012001. IOP Publishing.

Thorpe, S., 1977. Turbulence and mixing in a Scottish Loch. *Philos. Trans. R. Soc. London. Ser. A, Math. Phys. Sci.* 286: 125–181.

Tillinger, D. & Gordon, A.L., 2009. Fifty Years of the Indonesian Throughflow. *J. Clim.* 22: 6342–6355. doi: 10.1175/2009jcli2981.1

Tsuchiya, M., Lukas, R., Fine, R.A., Firing, E. & Lindstrom, E., 1989. Source waters of the Pacific Equatorial Undercurrent. *Prog. Oceanogr.* 23: 101–147. doi: 10.1016/0079-6611(89)900 12-8

Wyrtki, K., 1961. Physical oceanography of Southeast Asian waters. Naga Report 2.

Yang, L., Zhou, L., Li, S. & Wei, Z., 2018. Spreading of the South Pacific Tropical Water and Antarctic Intermediate Water Over the Maritime Continent. *J. Geophys. Res. Ocean.* 123(6): 4423-4446. doi: 2018JC013831